High-pressure phase transition of cesium chloride and cesium bromide

ARTICLE *in* PHYSICAL CHEMISTRY CHEMICAL PHYSICS · JULY 2014

Impact Factor: 4.49 · DOI: 10.1039/c4cp02452d · Source: PubMed

6 AUTHORS, INCLUDING:

Quan Li
Jilin University
61 PUBLICATIONS **806** CITATIONS

SEE PROFILE

PCCP

PAPER

View Article Online
View Journal | View Issue

Cite this: *Phys. Chem. Chem. Phys.*, 2014, **16**, 17924

High-pressure phase transition of cesium chloride and cesium bromide

Shubo Wei,[a] Chunye Zhu,[a] Qian Li,[a] Yuanyuan Zhou,[a] Quan Li*[ab] and Yanming Ma[ac]

Received 4th June 2014,
Accepted 9th July 2014

DOI: 10.1039/c4cp02452d

www.rsc.org/pccp

The high-symmetry cubic cesium chloride (CsCl) structure with a space group of $Pm\bar{3}m$ (Z = 1) is one of the prototypical AB-type compounds, which is shared with cesium halides and many binary metallic alloys. The study of high-pressure evolution of the CsCl phase is of fundamental importance in helping to understand the structural sequence and principles of crystallography. Here, we have systematically investigated the high-pressure structural transition of cesium halides up to 200 GPa using an effective CALYPSO algorithm. Strikingly, we have predicted several thermodynamically favored high-pressure phases for cesium chloride and cesium bromide (CsBr). Further electronic calculations indicate that CsCl and CsBr become metallic *via* band-gap closure at strong compression. The current predictions have broad implications for other AB-type compounds that likely harbor similar novel high-pressure behavior.

I. Introduction

Cesium halides are the simplest and most representative ionic solids, which have always been the subject of extensive theoretical and experimental studies.[1–17] Cesium halides adopt a prototypical cesium chloride (CsCl) structure with two-atom per primitive cubic lattice. Using energy-dispersive X-ray diffraction (XRD), a tetragonal phase of CsCl was observed at a pressure of 65 ± 5 GPa (the detailed crystal information is unsettled),[12] while cesium bromide (CsBr) was found to undergo a second-order phase transition to the tetragonal CuAu–I structure at 53 GPa.[15] Subsequently, experimental XRD measurements proposed that CsBr changed from a simple cubic phase to a tetragonal phase at a pressure of about 53 GPa.[16] However, subsequent first-principles calculations suggested a cubic-to-orthorhombic transition for CsX (X = Cl, Br and I) occurring at high pressure.[6] Recently, the structural sequence of $Pm\bar{3}m$ → *Pmma* → *Pnma* of CsI has been identified using evolutionary methodology and first principles calculations.[8] CsI metallizes at 115 GPa and becomes a superconductor above 180 GPa.[8] Although these experimental and theoretical studies have been devoted to the understanding of the high-pressure transition of CsCl and CsBr, the full high-pressure structural information is still far from being clear and well established. Previous experimental and theoretical attempts have mostly used empirical approaches for selecting and modifying known crystal structures to fit the experimental data or for simple comparison of the enthalpies of CsCl and CsBr. The proposed structures with X substituting for Y atoms of CsCl and CsBr are based on the knowledge of known chemically related AB-type structures; however, there is a possibility that some unknown structures are energetically stable instead. These structural uncertainties have impeded an in-depth understanding and further exploration of the structural sequence and principles of crystallography. It is greatly desirable to explore the phase transitions and the corresponding electronic properties of CsCl and CsBr under high pressure.

Here, we present an extensive structure search to uncover the high-pressure structures of CsCl and CsBr using the developed CALYPSO method,[18–21] which is very successful in predicting the high-pressure phase of materials.[22–29] Our work shows that CsCl and CsBr have the simple $Pm\bar{3}m$ structure at ambient pressure and undergo complicated transitions to low symmetric phases at high pressure. We have identified two thermodynamically stable orthorhombic *Pmma* and *Pbam* phases for CsCl and an orthorhombic *Pmma* phase for CsBr. The current *Pmma* phase of CsBr is energetically much superior to the previously proposed CuAu–I-type ($P4/mmm$) structure.[15] The present work establishes the comprehensive understanding of the high-pressure evolution of the structural properties of CsCl and CsBr. Our findings represent a significant step toward the understanding of the behavior of AB-type compounds under extreme conditions.

[a] *State Key Laboratory of Superhard Materials, Jilin University, Changchun 130012, China. E-mail: liquan777@jlu.edu.cn; Tel: +86-431-85167557*
[b] *College of Materials Science and Engineering, Jilin University, Changchun 130012, China*
[c] *Beijing Computational Science Research Center, Beijing 10084, China*

II. Calculation methods

We carried out a structural search using a global minimization of free energy surfaces based on the CALYPSO (Crystal structure

AnaLYsis by Particle Swarm Optimization) methodology and the first-principles calculations.[18–21] The remarkable feature of this methodology is the capability of predicting the stable structure with only the knowledge of the chemical composition under given external conditions (for example, pressure). The underlying *ab initio* structural relaxations and electronic calculations have been carried out using density functional theory within the Perdew–Burke–Ernzerhof generalized gradient approximation (PBE-GGA)[30] exchange correlation as implemented in the VASP (Vienna *ab initio* simulation package) code.[31] The projector augmented wave method (PAW) has been adopted, with $5s^2 5p^5 6s^1$, $3s^2 3p^5$ and $4s^2 4p^5$ treated as valence electrons for Cs, Cl and Br, respectively. The cutoff energy of 400 eV for the expansion of the wave function into plane waves and fine Monkhorst–Pack k meshes of 0.025 $Å^{-1}$ have been chosen to ensure that all the enthalpy calculations are well converged. The accuracy of the total energies obtained within the framework of density functional theory is in many cases sufficient to predict the stability of structures. The phonon calculations have been carried out by using a supercell approach as implemented in the PHONOPY code.[32] This method uses the forces obtained from the Hellmann–Feynman theorem and calculated from the optimized $3 \times 3 \times 3$ supercell. The Reflex Tools of Materials Studio code was used to simulate the X-ray diffraction data.[33]

III. Results and discussion

Structural predictions of CsCl and CsBr have been performed using CALYPSO methodology[18–21] and using simulation sizes with 1–4 formula per primitive cell at 0, 60, 80, 100, 120 and 200 GPa. According to our simulations, at 0 GPa, both the CsCl and CsBr adopt a cubic cesium chloride structure with a space group of $Pm\bar{3}m$, which is in good agreement with the experimentally known information.[3,4,10,12,15] The $Pm\bar{3}m$ structure adopts a two-atom primitive cubic lattice, where both atoms have eightfold coordination. The chloride atoms lie upon the lattice points at the edges of the cube, while the cesium atoms lie in the holes in the center of the cubes. For CsCl, the optimized lattice parameter of the $Pm\bar{3}m$ phase at 0 GPa is a = 4.209 Å, which is in good agreement with the experimental data of a = 4.123 Å.[10] This difference of 2.086% is owing to PBE-GGA exchange correlation, which tends to overestimate lattice parameters. For CsBr, the optimized structural parameter of the $Pm\bar{3}m$ structure is a = 4.391 Å, and is about 2.235% larger than experimental data of a = 4.295 Å.[10]

Here, two orthorhombic structures of CsCl with *Pmma* and *Pbam* symmetry are found under high-pressure, as shown in Fig. 1. Both *Pmma* and *Pbam* structures can also be viewed as a distorted CsCl structure. The lattice parameters and atomic coordinates derived from structural optimization are listed in Table 1. Fig. 2 shows the simulated X-ray diffraction data of these structures, indicating that their structures are different from each other. The enthalpy curves of the current predicted CsCl structures are shown in Fig. 3(a). It can be seen clearly that CsCl undergoes a phase transition from the cubic CsCl phase to the orthorhombic *Pmma* phase at 73.5 GPa. The current predicted transition pressure point (~73 GPa) is in excellent agreement with 65 ± 5 GPa obtained from earlier experiments.[12] The volume ratio of V/V_0 = 0.474 (V_0 being the equilibrium volume) is close to experimental data of 0.51 at transition pressure.[12] Compared with the cubic $Pm\bar{3}m$ structure, a striking

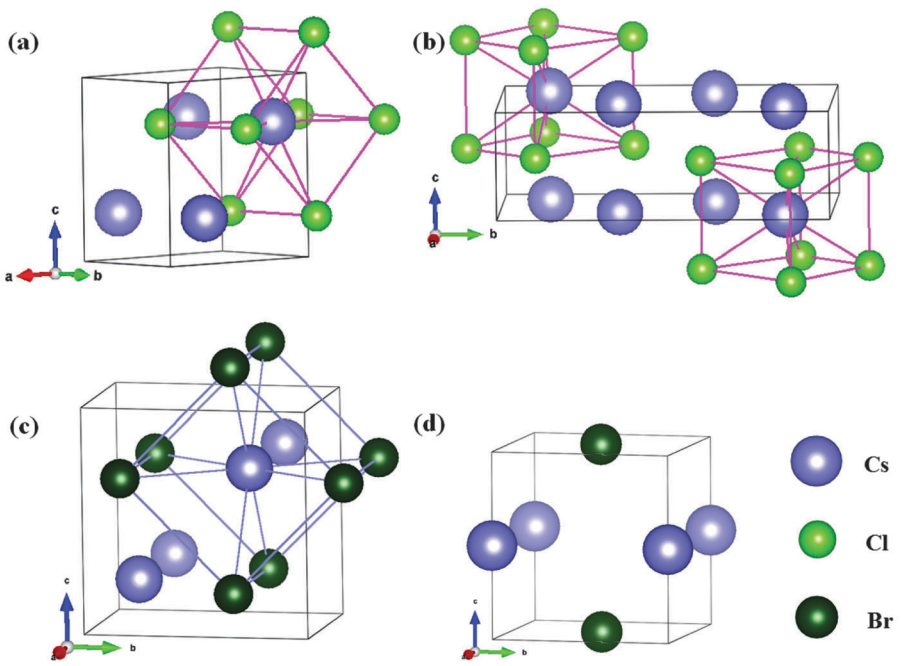

Fig. 1 The crystal structure of orthorhombic *Pmma* CsCl (a), *Pbam* CsCl (b), *Pmma* CsBr (c) and tetragonal *P4/mmm* CsBr (d).

Table 1 Lattice parameters and atomic coordinates of CsCl and CsBr

Phase	Lattice parameters (Å)	Atoms	*x*	*y*	*z*
Pmma CsCl 100 GPa	*a* = 4.491 *b* = 3.179 *c* = 4.492	Cs(2e) Cl(2f)	0.25 0.25	0.0 0.5	0.751 0.251
Pbam CsCl 200 GPa	*a* = 4.327 *b* = 8.578 *c* = 2.796	Cs(4g) Cl(4h)	0.811 0.192	0.861 0.391	0.0 0.5
Pmma CsBr 100 GPa	*a* = 4.731 *b* = 3.025 *c* = 4.851	Cs(2e) Br(2f)	0.25 0.25	0.0 0.5	0.804 0.307

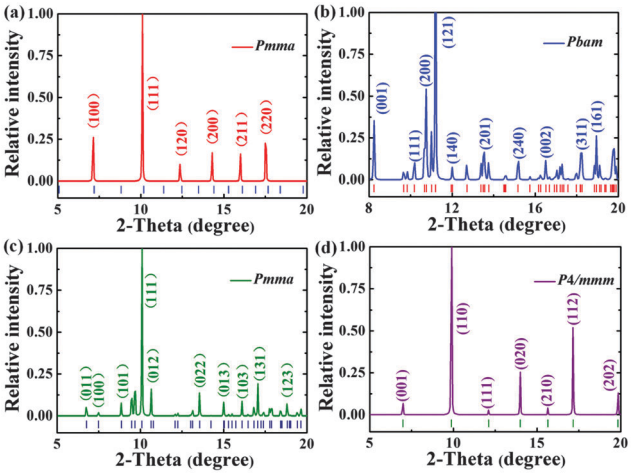

Fig. 2 The simulated power X-ray diffraction (λ = 0.407 Å and the diffraction data are obtained from powder diffraction and not single crystal) for *Pmma* CsCl at 80 GPa (a), *Pbam* CsCl at 185 GPa (b), *Pmma* CsBr at 80 GPa (c) and *P4/mmm* CsBr at 80 GPa (d).

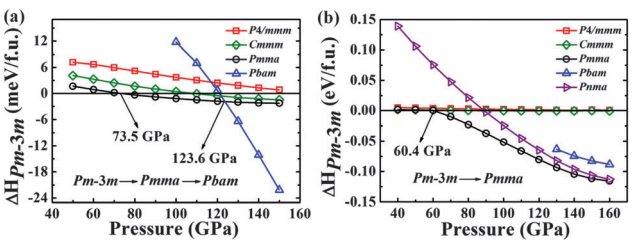

Fig. 3 (a) Enthalpies (related to the $Pm\bar{3}m$ phase) of *P4/mmm*, *Cmmm*, *Pmma* and *Pbam* structures of CsCl as a function of pressure. (b) Enthalpies (related to the $Pm\bar{3}m$ phase) of *P4/mmm*, *Cmmm*, *Pmma*, *Pbam* and *Pnma* structures of CsBr as a function of pressure.

feature of this modification is that Cs and Cl atoms are packed in a distortion structure, which results in breaking the symmetry to form the orthorhombic *Pmma* phase. The *Pmma* structure is stable in a wide pressure region of 73.5–123.6 GPa. Above that, CsCl undergoes further transition and transforms into the orthorhombic *Pbam* phase (Fig. 1(b)), which becomes favorable and remains stable up to at least 200 GPa (Fig. 3(a)). Therefore, the high-pressure transition phase order is $Pm\bar{3}m \rightarrow Pmma \rightarrow Pbam$ for CsCl from thermodynamics. Moreover, we have compared the enthalpies of these two new orthorhombic phases of CsCl with the *P4/mmm* and *Pnma* structures, which increased previously for CsBr and CsI, respectively.[8,15] The calculated enthalpy differences confirm that the *Pmma* phase is lower than *P4/mmm* and *Pnma* phases. The enthalpy curve of *Pnma* is not shown due to its high enthalpy. In fact, the *Pmma* structure should be viewed as a symmetry-breaking structure ($a \neq c$) in the orthorhombic subgroups of the tetragonal *P4/mmm* structure. Noticeably, the lattice parameter *a* = 4.491 Å of *Pmma* CsCl is extremely close to *c* = 4.492 Å and the deviations from the ideal *z* coordinates for both Cs and Cl (0.75 and 0.25, respectively) are very small (Table 1). The group–subgroup relationships indicate that the *Pmma* structure could be transformed into *Cmmm* or *P4/mmm* phases, however *Cmmm* and *P4/mmm* phases do not possess thermodynamic stability in the entire pressure range (Fig. 3(a)). And, when the *b* lattice parameter is multiplied by a square root of 2, the resulting number 4.496 Å is very close to the *a* and *c* parameters. This indicates that the calculated structure is highly pseudo-symmetric. In addition, the space groups *Pmma* and *Pbam* for CsCl at 100 GPa and 200 GPa, respectively, are related to each other. Assuming that the lattice parameters and the atomic positions of the Cs and Cl atoms are in space group *Pbam*, a structure in space group *Pmma* using a group–subgroup relationship could be obtained with *a* = 4.327 Å, *b* = 2.796 Å, and *c* = 4.289 Å. The new atomic positions, Cs(2e) (0.25, 0, and 0.278) and Cl(2f) (0.75, 0.5, and 0.218), are very close to those for these atoms at 100 GPa (Table 1). It is clearly the case of a highly pseudo-symmetric structure that exists at high pressures, *i.e.*, the structure in space group *Pbam* is a superstructure of the phase in *Pmma*. From the pressure evolution of the lattice parameters and *z* coordinates of CsCl (Fig. 4), the deviations of *a* with *c* parameters and *z* coordinates with the ideal *z* coordinates of *Pmma* CsCl are small due to its highly pseudo-symmetric feature. The lattice dynamics calculations with no imaginary phonon frequencies support the

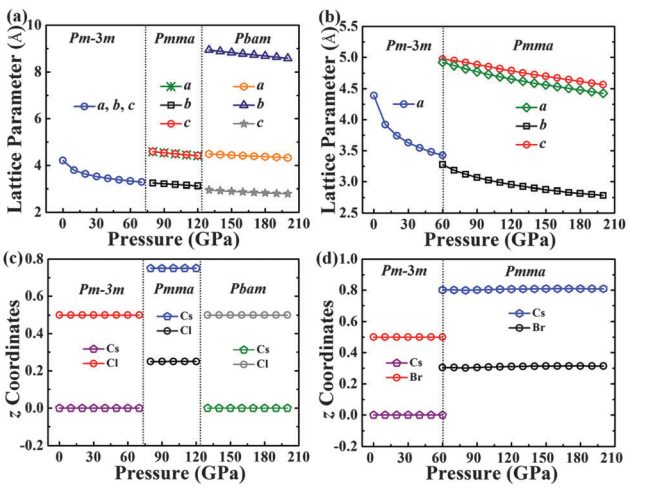

Fig. 4 The pressure evolution of the lattice parameters of CsCl (a) and CsBr (b). The pressure evolution of the *z* coordinates of CsCl (c) and CsBr (d).

dynamic stability of *Pmma* and *Pbam* structures over the pressure range studied here (Fig. 5).

From the enthalpy curves of CsBr for various structures (Fig. 3(b)), the transformation from the $Pm\bar{3}m$ to *Pmma* structure (Fig. 1(c) and Table 1) is predicted at 60 GPa. Our calculations show that *Pmma* remains stable up to at least 200 GPa. Earlier experiments suggested that CsBr undergoes a tetragonal *P4/mmm* distortion at 53 GPa.[15] However, we can see that the enthalpy of our predicted *Pmma* structure is 13.5 meV per CsBr lower than that of the *P4/mmm* structure at 70 GPa (Fig. 3(b)), indicating that the *P4/mmm* structure is thermodynamically unstable. Moreover, the *Pmma* phase is also more stable than *Pbam* CsCl, *Pnma* CsI and *Cmmm* structures (Fig. 3(b)). As shown in Fig. 2, the simulated XRDs with different diffraction peaks also support the observation that the current orthorhombic *Pmma* phase is geometrically different from the previously proposed tetragonal *P4/mmm* structure. No imaginary frequencies are observed throughout the whole Brillouin zone, indicating that this *Pmma* phase of CsBr at the studied pressure region is dynamically stable (Fig. 5(c)).

Previous calculations suggested that CsI becomes metallic *via* band-gap closure at strong compression (>100 GPa).[8] Thus, it is intriguing to determine whether CsCl and CsBr will become metallic in the same way. The calculated electronic band structures of *Pmma* CsCl at 123 GPa (Fig. 5(d)) show that it is a narrow band gap semiconductor with a direct band-gap of 0.82 eV at the Γ point. As shown in Fig. 6, our calculated electronic band structures show that the band gaps of CsCl and CsBr are sensitive to the change in external pressure (decreasing volume). As the pressure increases, the sizes of the band gaps have negative pressure dependence. Interestingly, CsCl becomes metallic *via* band-gap closure at ~170 GPa (Fig. 5(e)). The metallization of *Pbam* CsCl occurs *via* direct band-gap closure at the Γ point, which is similar to that of *Pnma* CsI (*via* indirect band-gap closure along the Z–Γ and Γ–Y directions).[8] Similarly, *Pmma* CsBr becomes metallic *via* direct band-gap closure at the Γ point (Fig. 5 and 6) at ~150 GPa. Pressure induces CsX to exhibit increasingly shorter interatomic distances, which is accompanied by an increase in the bandwidth, especially those near the Fermi-surface, thus leading

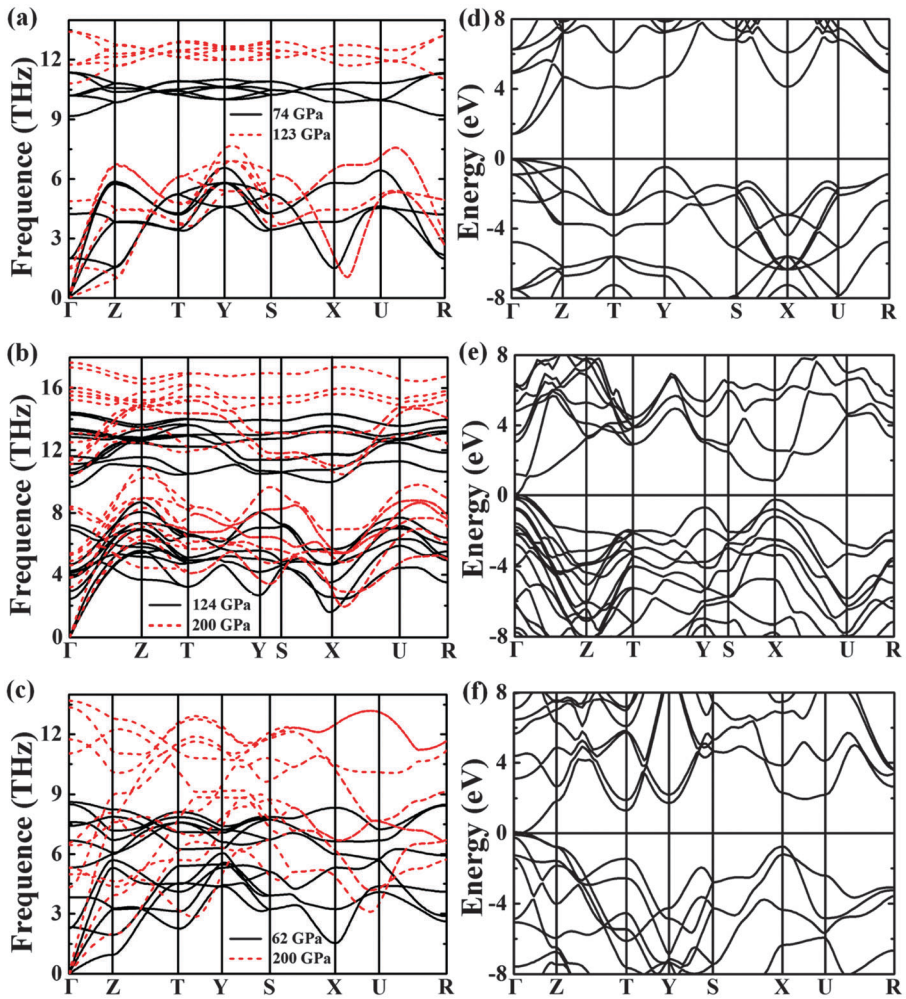

Fig. 5 Calculated phonon spectrum of *Pmma* CsCl at 74 and 123 GPa (a), *Pbam* CsCl at 124 and 200 GPa (b) and *Pmma* CsBr at 62 and 200 GPa (c). Calculated electronic band plot along high-symmetry directions of *Pmma* CsCl at 123 GPa (d), *Pbam* CsCl at 170 GPa (e) and *Pmma* CsBr at 160 GPa (f).

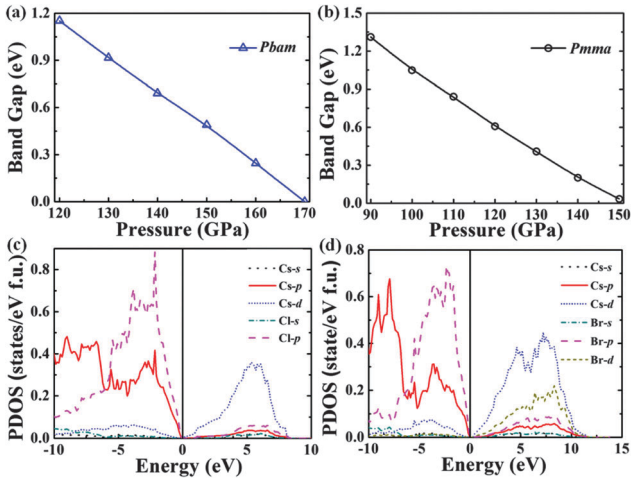

Fig. 6 Pressure dependence of theoretical band gaps of *Pbam* CsCl (a) and *Pmma* CsBr (b). Electronic density of states of *Pbam* CsCl at 170 GPa (c) and *Pmma* CsBr at 160 GPa (d).

to the metallic nature of CsX. It should be mentioned that the superconducting behaviors in CsI have been extensively explored through experimental measurements and theoretical calculations.[8,34,35] It is suggested that the formation of several electrons and hole Fermi-surface pockets in CsI is due to a dramatic increase of the electron donation from I^- to Cs^+, thus leading to more electrons to be involved in the EPC, which is responsible for superconducting and the larger electron-phonon coupling potential, thereby contributing to the increase in T_c.[8] Thus, those metallic CsCl and CsBr phases would also undergo superconducting transition; however, the studies of superconducting T_c are beyond the scope of this work.

IV. Conclusions

Using the CALYPSO method for crystal structure prediction combined with first-principles calculations, we have investigated the high-pressure crystal structures and established the corresponding phase boundaries for the prototypical AB-type compounds of CsCl and CsBr. Two orthorhombic phases for CsCl with the space groups of *Pmma* and *Pbam* and an orthorhombic *Pmma* phase for CsBr are predicted to be energetically much superior to the previously proposed tetragonal CuAu–I-type structure. *Pbam* CsCl and *Pmma* CsBr become metallic with band-gap narrowing due to the expansion of the bandwidth induced by pressure, analogous to what was previously reported for CsI. This work presents significant meaning concerning the fundamental structural properties of the simplest and the most representative ionic solid material with implications for an entire family of similar materials.

Acknowledgements

This work was supported by the China 973 Program (2011CB808200), the Natural Science Foundation of China under No. 11274136, 11025418, 51202084, 11104104 and 91022029, the 2012 Changjiang Scholars Program of China, Changjiang Scholar and Innovative Research Team in University (IRT1132). Parts of the calculations were performed in the High Performance Computing Center (HPCC) of Jilin University.

References

1 E. Madelung, *Phys. Z.*, 1918, **19**, 524.
2 P. O. Ewald, *Ann. Phys.*, 1921, **64**, 253.
3 T.-L. Huang and A. L. Ruoff, *Phys. Rev. B: Condens. Matter Mater. Phys.*, 1984, **29**, 1112.
4 T.-L. Huang, K. E. Brister and A. L. Ruoff, *Phys. Rev. B: Condens. Matter Mater. Phys.*, 1984, **30**, 2968.
5 Q. Williams and R. Jeanloz, *Phys. Rev. Lett.*, 1987, **59**, 1132.
6 M. B. Nardelli, S. Baroni and P. Giannozzi, *Phys. Rev. B: Condens. Matter Mater. Phys.*, 1995, **51**, 8060.
7 H. Pattyn, M. M. Abd-Elmeguid, S. Bukshpan, K. Milants and J. Verheyden, *Phys. Rev. B: Condens. Matter Mater. Phys.*, 1995, **51**, 10357.
8 Y. Xu, J. S. Tse, A. R. Oganov, T. Cui, H. Wang, Y. Ma and G. Zou, *Phys. Rev. B: Condens. Matter Mater. Phys.*, 2009, **79**, 144110.
9 V. Sharma, S. Tiwari and B. L. Ahuja, *Radiat. Phys. Chem.*, 2010, **79**, 678–686.
10 E. Henry, *Solid state physics: advances in research and applications*, Academic Press, 1984, vol. 29, p. 31.
11 E. Knittle and R. Jeanloz, *J. Phys. Chem. Solids*, 1985, **46**, 1179.
12 K. E. Brister, Y. K. Vohra and A. L. Ruoff, *Phys. Rev. B: Condens. Matter Mater. Phys.*, 1985, **31**, 4657.
13 Y. K. Vohra, K. E. Brister, S. T. Weir, S. J. Duclos and A. L. Ruoff, *Science*, 1986, **231**, 1136.
14 E. Knittle and R. Jeanloz, *Science*, 1984, **223**, 53–56.
15 E. Knittle, A. Rudy and R. Jeanloz, *Phys. Rev. B: Condens. Matter Mater. Phys.*, 1985, **31**, 588.
16 L. Wang, L. Chen, F. Li, H. Gu, L. Zhou and R. Che, *Chin. Phys. Lett.*, 1998, **15**, 284.
17 S. Satpathy, *Phys. Rev. B: Condens. Matter Mater. Phys.*, 1986, **33**, 8706.
18 Y. Wang, J. Lv, L. Zhu and Y. Ma, *Comput. Phys. Commun.*, 2012, **183**, 2063–2070. CALYPSO Code is Free for Academic Use. Please Register at http://www.calypso.cn.
19 Y. Wang, J. Lv, L. Zhu and Y. Ma, *Phys. Rev. B: Condens. Matter Mater. Phys.*, 2010, **82**, 094116.
20 Y. Wang, M. Miao, J. Lv, L. Zhu, H. Liu and Y. Ma, *J. Chem. Phys.*, 2012, **137**, 224108.
21 J. Lv, Y. Wang, L. Zhu and Y. Ma, *J. Chem. Phys.*, 2012, **137**, 084104.
22 F. Peng, M. Miao, H. Wang, Q. Li and Y. Ma, *J. Am. Chem. Soc.*, 2012, **134**, 18599.
23 H. Wang, J. S. Tse, K. Tanaka, T. Iitaka and Y. Ma, *Proc. Natl. Acad. Sci. U. S. A.*, 2012, **109**, 6463.
24 L. Zhu, Z. Wang, Y. Wang, G. Zou, H. K. Mao and Y. Ma, *Proc. Natl. Acad. Sci. U. S. A.*, 2012, **109**, 751.
25 Q. Li, D. Zhou, W. Zheng, Y. Ma and C. Chen, *Phys. Rev. Lett.*, 2013, **110**, 136403.

26 C. Lu, M. Miao and Y. Ma, *J. Am. Chem. Soc.*, 2013, **135**, 14167.
27 Q. Li, H. Liu, D. Zhou, W. Zheng, Z. Wu and Y. Ma, *Phys. Chem. Chem. Phys.*, 2012, **14**, 13081.
28 S. Lu, Y. Wang, H. Liu, M. Miao and Y. Ma, *Nat. Commun.*, 2014, **5**, 3666.
29 L. Zhu, H. Liu, C. J. Pickard, G. Zou and Y. Ma, *Nat. Chem.*, 2014, **6**, 644–648.
30 J. P. Perdew, K. Burke and M. Ernzerhof, *Phys. Rev. Lett.*, 1996, **77**, 3865.
31 G. Kresse and J. Furthmuller, *Phys. Rev. B: Condens. Matter Mater. Phys.*, 1996, **54**, 11169.
32 A. Togo, F. Oba and I. Tanaka, *Phys. Rev. B: Condens. Matter Mater. Phys.*, 2008, **78**, 134106.
33 Forcite Module, *Material Studio 6.0*, Accelrys Inc., San Diego, CA, 2011.
34 M. I. Eremets, K. Shimizu, T. C. Kobayashi and K. Amaya, *Science*, 1998, **281**, 1333.
35 M. I. Eremets, K. Shimizu, T. C. Kobayashi and K. Amaya, *J. Phys.: Condens. Matter*, 1998, **10**, 11519.